Indian Journal of Pure & Applied Physics
Vol. 53, July 2015, pp. 456-463

Study of structural, electrical and thermal properties of polyaniline/ZnO composites synthesized by *in- situ* polymerization

Sneh Lata Goyal*, Smriti Sharma, Deepika Jain & N Kishore

Department of Applied Physics, Guru Jambheshwar University of Science and Technology, Hisar 125 001, Haryana, India

*E-mail: goyalsneh@yahoo.com

Received 23 December 2014; revised 2 March 2015; accepted 16 April 2015

This paper reports the structural, electrical and thermal properties of the polyaniline doped with ZnO composites. Conducting polymer composites of polyaniline/zinc oxide (PANI/ZnO) have been synthesized by *in-situ* polymerization of aniline using various compositions (10, 20, 30, 40, 50 wt %) of ZnO in PANI using ammonium persulphate as an oxidant. The amorphous nature of the composites has been ascertained by the X-ray diffraction. Fourier Transform Infrared (FTIR) spectroscopy confirms the interaction between PANI and dopant. Thermal stability of polymer composites has been analyzed by TGA and corresponding thermal kinetic parameters were calculated using Horowitz-Metzger method. Thermal analysis shows higher thermal stability of PANI/ZnO composites than pure PANI. The surface morphology of these composites was analyzed with Scanning Electron Microscopy (SEM), which also confirms the presence of ZnO in the composites. The *dc* conductivity behaviour of these composites has also been investigated as a function of temperature and concentration in the temperature range 313-393 K and the results were compared with pure PANI. The *dc* electrical conductivity of PANI/ZnO composites decreased as the ZnO content increased in PANI but increased with the increase in temperature.

Keywords: Polyaniline, Thermal analysis, Scanning electron microscopy, XRD

1 Introduction

Intrinsically conducting polymers have attracted researchers in field of material science due to their promising and unique electrical properties such as energy storage devices[1], gas sensors[2], electromagnetic interference shielding[3-10], electrostatic charge dissipation, light emitting diodes and flexible display devices[11], anti-corrosive material[12], electrochromic materials[13] and electronic conducting fabrics[14]. The electrical transport in polymeric materials has become an area of increasing interest in research because of the fact that these materials have great potential for solid state devices. Similarly, conducting polymer composites attracted considerable interest in recent years because of their numerous applications in variety of electric and electronic devices. Conducting polymer composites with proper compositions of one or more insulating materials results into desirable properties[15]. Although presently, a number of conducting polymers have been synthesized, but polyaniline is the most important conducting polymer due to its high conductivity, ease of preparation, low cost and good environmental and thermal stability[16]. Later on, it was shown that the conductivity of these polymers changes significantly upon doping. The attractive electro-chemical and physico-chemical properties result in polyaniline having various practical applications, including electrochromic devices, electrochemical super capacitors, batteries, biosensors and corrosion inhibitors. ZnO is a semiconducting material that has direct wide band gap (3.37 eV) and large excitation binding energy (60 meV) at room temperature[17,18]. ZnO is a non-toxic material and *n*-type semiconductor with a good photocatalytic activity. Indeed ZnO is a peculiar material that exhibits multiple properties that include piezoelectric, semiconducting and pyroelectric characters. As a consequence, now-a-days, there is an increased demand for use of ZnO in different applications such as active materials in batteries[19], photo detectors[20], biosensors[21], optoelectronic[22] and photovoltaic devices[23].

In the present paper, PANI/ZnO composites were prepared by *in -situ* polymerization of aniline monomer with ZnO. The characterization of the composites with different doping concentrations is reported. All these composites have been analyzed using X-ray diffraction (XRD), SEM, FTIR spectroscopy and thermal analysis. The variation in *dc* conductivity of these composites was also studied as a

function of temperature and concentration. Through doping of ZnO in PANI components, the goals of this research are to create a useful compound with valuable physical characteristics and a new noble material which can be utilized for electric and bio-sensing applications.

2 Experimental Details

2.1 Preparation of PANI

All Chemicals used were procured from sigma aldrich and used as received. To prepare PANI, 0.2 M aniline hydrochloride and 0.25 M ammonium persulphate (APS) solutions were prepared in distilled water. Both solutions were left to cool for 1-2 h in refrigerator. Pre-cooled APS is added drop wise in aniline hydrochloride solution, maintained at a temperature in the range 0-4°C in an ice bath, stirred for 2 h for oxidization and left for 24 h at rest to polymerize in refrigerator. Next day PANI precipitate was collected on a filter paper and washed with the 200 ml of 1M HCl and acetone till the filtrate became colourless. PANI (emeraldine) hydrochloride powder was dried in air and then in vacuum at 45°C. Polyaniline prepared under these conditions was taken as standard sample.

2.2 Preparation of PANI/ZnO composites

The sample of PANI and zinc oxide composite was prepared by adding 0.1 M solution of 10 wt % of zinc oxide (dopant) to 0.2 M aniline hydrochloride (monomer) solution in distilled water. The solution was vigorously stirred for 1 h in order to keep the zinc oxide suspended in the solution. Also 0.25 M ammonium persulphate (APS) solution was prepared in distilled water. All the solutions were pre-cooled before mixing. The aqueous solution of APS (0.25 M) was added drop wise in the beaker containing the mixed solution of monomer and dopant, maintained at temperature in the range 0-4°C in an ice bath. Then this solution was stirred for 2 h for oxidization and left for 24 h at rest to polymerize in refrigerator. Next day precipitate of the composite of PANI/zinc oxide was collected on a filter paper and washed with the 200 ml of 1M HCl and acetone till the filtrate became colourless. Precipitate of the sample was dried in air and then in vacuum at 45°C. Following this procedure, five different samples of PANI/zinc oxide composites with 10, 20, 30, 40, 50 wt% of zinc oxide were prepared and named as Z1, Z2, Z3, Z4 and Z5.

2.3 Analytical techniques

The samples were characterized by XRD, FTIR, TGA techniques, SEM and *dc* conductivity. XRD studies of the samples were performed by using Rigaku Table-Top X-ray diffractometer. FTIR analysis was done by using Shimadzu IR affinity-1 8000 FTIR spectrometer by mixing the powder sample with dry KBr. TGA analysis was performed by TA instrument, model no. SDT Q600 in nitrogen atmosphere with a heating rate of 10°C/min. SEM was done using Microtrac Semtrac Mini SM-300. *DC* conductivity measurements were made by using Keithley 6517B electrometer.

3 Results and Discussion

3.1 XRD analysis

The XRD patterns of the pure zinc oxide, PANI/ZnO composites and pure PANI are shown in Figs 1 and 2, respectively. PANI/ZnO composites consist of a few broad peaks. It shows that the XRD patterns of all the composites are similar and all are similar to the one reported in literature for pure PANI. XRD pattern of polyaniline has broad band at a value of 2θ about 25 degrees. XRD pattern of zinc oxide has sharp peak of maximum intensity at 36·25° along with certain other peaks of low intensity. By comparing the XRD pattern of composites with that of ZnO, it is observed that prominent peaks correspond to 2θ = 31·77°, 34·22°, 36·25°,47·53°, 56·60°, 62·86°, 67·96° and are due to (100), (002), (101), (102), (110), (103), (112) planes, respectively (JCPDS 36-1451) of pure ZnO is absent in XRD patterns of the PANI/ZnO composites. This may be

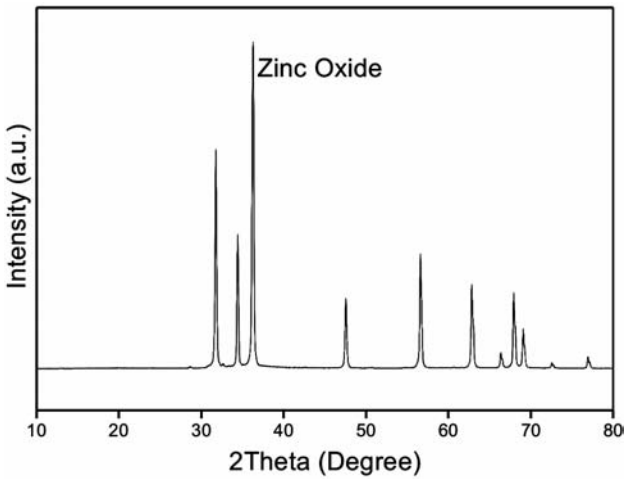

Fig. 1 — XRD of zinc oxide

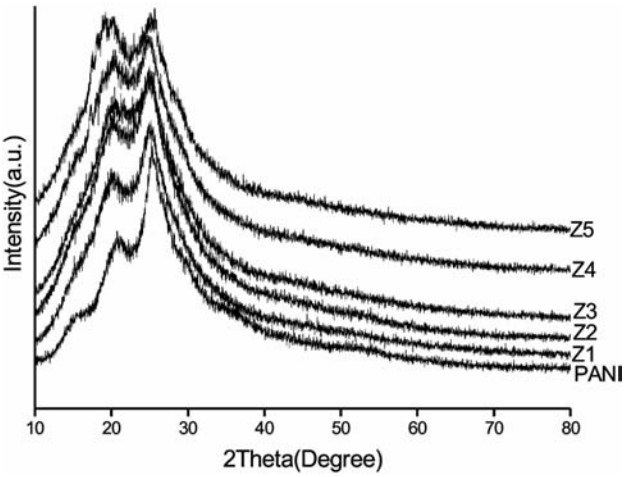

Fig. 2 — XRD pattern of PANI and PANI/ZnO composites

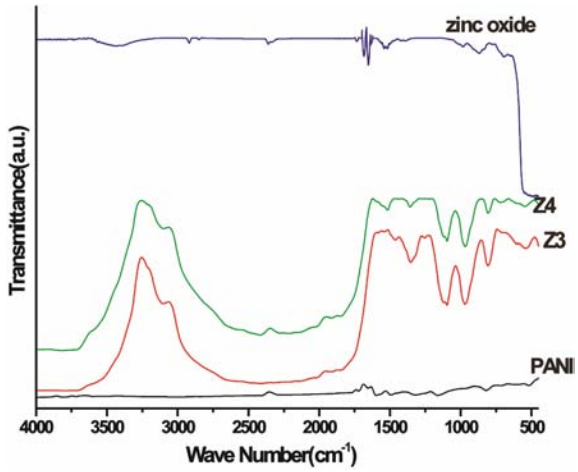

Fig. 3 — FTIR spectra of PANI, PANI/ZnO composites and ZnO

due to presence of zinc oxide in trace amount in composites. Present studies indicate hardly any effect of Zn^{2+} on the crystallinity of PANI/zinc oxide. This result is in agreement with those reported in the literature[24].

3.2 FTIR analysis

Figure 3 shows the FTIR spectra of pure PANI, PANI/ZnO and pure zinc oxide. The FTIR spectrum of pure PANI has characteristics bands at 520, 815, 1163, 1317, 1495 and 1589 cm^{-1}. C-H out- of -plane bending vibration and *para*-disubstituted benzene rings are shown by the bands at 520 and 815 cm^{-1}, respectively[25]. C-N stretching vibration is shown by band at1317 cm^{-1}. The peaks at 1163, 1495 and 1589cm^{-1} are attributed to, in-plane bending vibration in C-H, C- N and C- C stretching mode of vibration for the quinonoid and benzenoid units of PANI, respectively. Non-symmetric C_6 ring stretching modes are shown by the bands present in the range 1450-1600 cm^{-1}. The broad band observed at 2400-2750 cm^{-1} is due to aromatic C-H stretching vibrations while the band at 2950-3300 cm^{-1} is due to N-H stretching of aromatic amines. In composites, bands at 3763 cm^{-1} correspond to O-H stretching frequencies. The FTIR spectrum of ZnO shows the presence of bands around 3477 cm^{-1} and 1560 cm^{-1} which confirms the formation of pure ZnO compound. The band at 3477 cm^{-1} corresponds to the stretching vibrations of the OH group on the surface of ZnO particles[26]. The FTIR spectra of composites show that intensities of most of the peaks are affected by the presence of ZnO during polymerization of PANI.

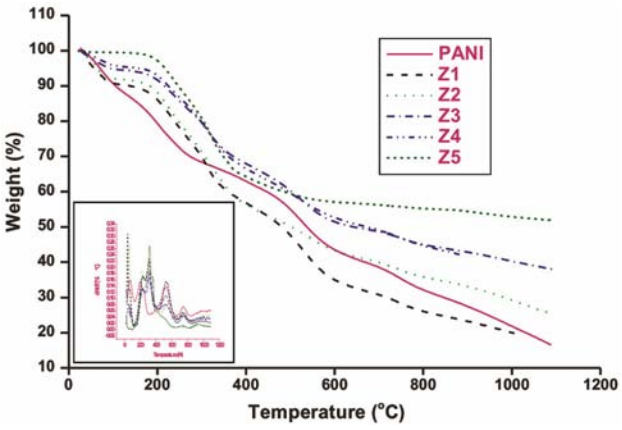

Fig. 4 — TGA and DTG (inset) thermo gram of PANI and PANI/ZnO composites

This can be explained on the basis of constrained growth and restricted modes of vibration in PANI grown in the presence of ZnO. In case of composites of PANI/zinc oxide, there exists small shifting in frequencies of PANI bands. In PANI/zinc oxide composites, the bands of zinc oxide are also visible. Thus, zinc oxide presence is confirmed by FTIR results.

3.3 Thermo gravimetric analysis

A TGA thermogram of PANI and PANI/ZnO composites in nitrogen atmosphere is shown in Fig. 4 and DTG thermogram is shown as inset in Fig. 4. The TGA and DTG analysis of PANI/ZnO composites indicate the four steps of weight loss. First stage starting at about 100°C is considered as initial dehydrating stage due to desorption of water absorbed at the surface of doped polymer. Second stage at

about 250°C is due to removal of protonic acid component. The following stages (third at about 500°C and fourth at about 600°C) indicate the polymer chain break which can lead to production of gases[27].

3.3.1 Activation energy

Horowitz-Metzger[28-33] method is used to determine the various kinetic parameters from TGA thermograms. The activation energy (E_a) of pure PANI and PANI/ZnO composites has been deduced using expression[33]:

$$\ln\left[\ln\left(\frac{w_0 - w_f}{w - w_f}\right)\right] = \frac{E_a \theta}{RT_s^2} \qquad \ldots(1)$$

where w_0 is the initial weight, w the remaining weight at temperature T, w_f the final weight, E_a the activation energy, R is gas constant and $\theta = T - T_s$ with T_s as the reference temperature corresponding to $[(w-w_f)/(w_0-w_f)]=1/e$. From Eq. (1), the activation energy E_a can be calculated from the slope of the linear fitted line between $\ln\{\ln[(w_0-w_f)/(w-w_f)]\}$ and θ as shown in Fig. 5 for pure PANI and PANI/ ZnO composites. The values of activation energy so obtained have been listed in Table 1. It is clear that the value of activation energy increases with increasing content of ZnO which signifies the increase in thermal stability of composites[34]. Higher thermal stability of composites as compared to PANI is due to more incorporation of inorganic component which may restrict the thermal motion of the PANI chain and shield the degradation of PANI in the composite[35].

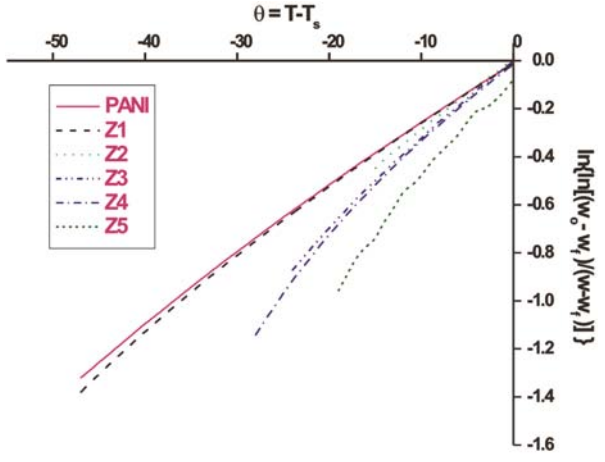

Fig. 5 — Plot of $\ln[\ln (w_0-w_f)/(w-w_f)]$ versus θ for PANI and PANI/ZnO composites

3.3.2 Frequency factor

Frequency factor (A) indicates the number of collisions which have the correct orientation to lead the products and is related to rate of reaction. The values of frequency factor for pure PANI and its composites with ZnO have been determined by substituting the values of activation energy (E_a) in the expression[33,36]:

$$A = \frac{\beta E_a}{RT_s^2} \exp\left(\frac{E_a}{RT_s}\right) \qquad \ldots(2)$$

where A is the frequency factor and β is the constant rate of heating and other letters have their usual meanings. The calculated values of frequency factor are listed in Table 1. It is clear that corresponding to the increase in values of activation energy, the values of frequency factor increase. The rate of reaction is increased with the increase in frequency factor.

3.3.3 Entropy of activation

Entropy of activation (ΔS) is the difference between the entropy of the transition state and the sum of the entropies of the reactants and is calculated as expreesion[33,36] below:

$$\Delta S = 2.303R \log\left(\frac{Ah}{kT_s}\right) \qquad \ldots(3)$$

where k is Boltzmann constant and h is Planck's constant and other letters have their usual meanings. The values of entropy of activation so calculated are listed in Table 1. The value of entropy of activation increases with the increase in doping concentration of ZnO which in turn suggests the increase in the rate of reaction. Also negative value of ΔS shows that the activated complex has more ordered structure than the reactants[36].

Table 1 — Values of various kinetic parameters for PANI and PANI/ZnO composites

Sample	E_a (KJ/mol)	$A(10^8)$ (s^{-1})	ΔS (J/mol/K)	ΔG (KJ/mol)
PANI	123.30	0.0040	-335.89	393.02
Z1	138.06	0.029	-298.11	381.02
Z2	164.09	0.48	-245.66	374.14
Z3	170.12	1.84	-219.54	354.54
Z4	183.28	18.28	-175.31	328.78
Z5	202.39	277.31	-123.32	305.25

3.3.4 Free energy of change of decomposition

The difference between the enthalpy of the transition state and the sum of the enthalpies of the reactants in the ground state is called free energy of change of decomposition (ΔG). ΔG is the driving force of a chemical reaction. Spontaneity of the reaction[33] is determined by ΔG.

The values of ΔG is determined by this expression[33,36]:

$$\Delta G = E_a - T_s \Delta S \qquad \ldots(4)$$

The values thus calculated are listed in Table 1. Non-spontaneity of the degradation reaction is shown by the positive value of ΔG.

3.4 Scanning Electron Microscopy (SEM)

SEM images of composites show that there is no agglomeration of zinc oxide particles in PANI matrix. In the micrographs of undoped PANI, relatively bigger size particles with weak bonding are observed (Fig. 6). While SEM of the composite with 40 wt% shows that interaction between particles in the composite has increased. The structures with bigger sized particles such as that seen for the undoped PANI could not be seen in Fig. 7 of the composite (40 wt%). SEM of PANI/ZnO composites shows the presence of micro crystallites which are uniformly distributed as shown in Fig. 7. The particle size comes out to be in micrometer range (≈ 3.885 μm).

3.5 *dc* conductivity

The powder of PANI and PANI/zinc oxide composites are crushed finely in agate pestle-mortar. This powder is pressed to form the pellets of 12 mm diameter and thickness ≈ 1 mm by applying pressure of 100 kg/cm^{-2} in a hydraulic press and coated with silver paste on both sides of the surfaces to obtain better contacts. Current (*I*)–voltage (*V*) characteristics of PANI/ZnO composite with 50 wt% of ZnO at various temperatures is shown in Fig. 8.

The current increases non-linearly with applied voltage in the conducting polymers and this behaviour is very much different from intrinsic semiconductors[37,38]. Under the influence of applied external field, the localized (short range) motions of the trapped charges in the sample serve as effective electric dipoles[39] which contribute to the formation of polarons and bipolarons. As the strength of the applied field increases, the degree of such distortion increases, resulting in the increment of current. It is also observed that the current increases with the

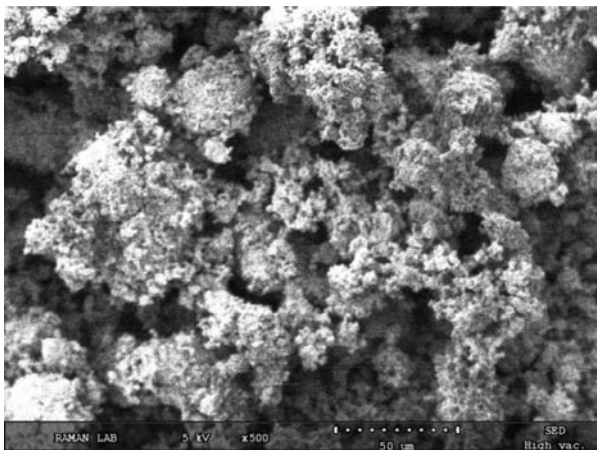

Fig. 6 — SEM micrograph of pure PANI

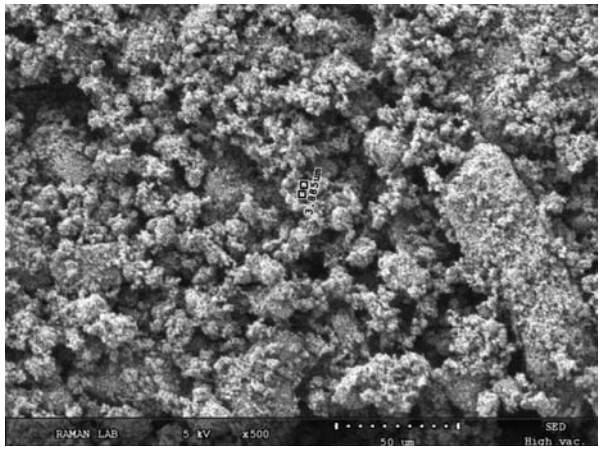

Fig. 7 — SEM micrograph of PANI/ZnO composite (40 wt %)

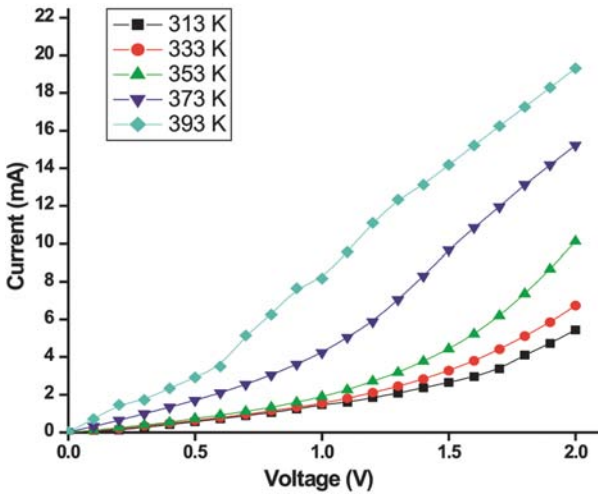

Fig. 8 — *I-V* characteristic of PANI /ZnO composite (50 wt%) at various temperatures

increase in temperature. Elevations in temperature lead to an increase in lattice vibration, which results in chain stretching[40]. It is known that PANI as emeraldine base (EB) is an insulator. Doping converts it from an insulator to a conductor/semiconductor. The conductivity of PANI is very much dependent on the nature of dopant. From the measured *I-V* characteristics of these samples, the values of *dc* electrical conductivities (σ) have been estimated by this formula at different temperatures at 0.5 V:

$$\sigma = \frac{I \times L}{V \times A} \qquad \ldots(5)$$

where I is the current, L the thickness, V the voltage and A is the area of cross -section of the sample. The *dc* conductivity decreases when doped with ZnO and also conductivity decreases with increasing content of ZnO in PANI/ZnO composites as mentioned in Table 2.

This decrease in conductivity by the addition of semiconducting ZnO may be due to the blocking of charge carriers to hop between favourable sites which in turn lower the overall conductivity of composite[38,41]. As shown in Fig. 9, *dc* electrical conductivity increases with increase in temperature. This may be due to increase in free charges with increase in temperature. The analysis of temperature dependent conductivity data suggests that the charge transport mechanism in PANI as well as all its composites can be explained by the variable range hopping (VRH) model[42] where dependence of *dc* conductivity is governed by expression:

$$\sigma(T) = \sigma_0 \exp\left[-\left(\frac{T_0}{T}\right)^{\gamma}\right] \qquad \ldots(6)$$

where T_0 is the characteristic temperature evaluated from linear slope of $\ln(\sigma_{dc})$ versus $T^{-\gamma}$ and associated with the degree of localization of the electronic wave function σ_0, the dc conductivity at absolute zero temperature and γ is the VRH exponent which depends upon the dimension of the system, where σ is the conductivity of the sample and T is the temperature. The exponent $\gamma=1/(1+d)$ determines the

Table 2 — DC conductivity of PANI and PANI/ZnO composites at various temperatures at 0.5 V

Temp	Conductivity (10^{-4}) (S/cm)					
	PANI	Z1	Z2	Z3	Z4	Z5
313	5.88	5.10	3.39	3.23	3.04	2.53
333	6.97	5.68	3.84	3.53	3.16	2.76
353	7.81	6.14	4.38	3.97	3.57	3.24
373	8.4	7.03	5.03	4.54	4.02	3.66
393	8.68	7.62	5.73	5.23	4.71	4.43

Table 3 — Values of $\ln\sigma_0$ and T_0

Sample	$\ln\sigma_0$ (S/cm)	T_0 (10^5) K
PANI	-0.5964	6.61
Z1	0.1513	11.264
Z2	1.7881	28.932
Z3	1.0487	21.842
Z4	0.5475	18.291
Z5	1.8972	34.569

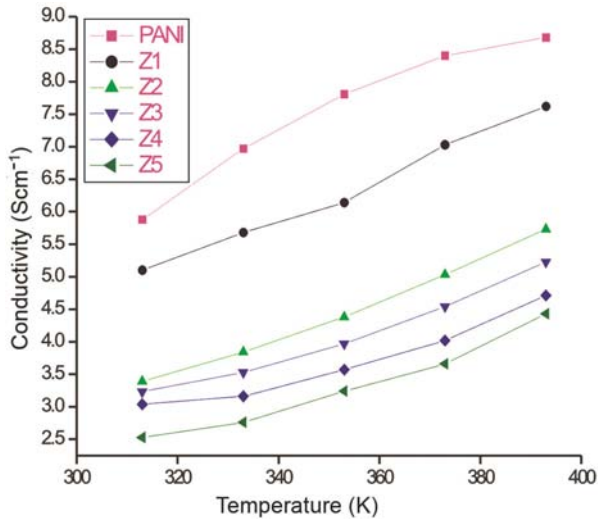

Fig. 9 — Conductivity of PANI and PANI/ZnO composites versus temperature

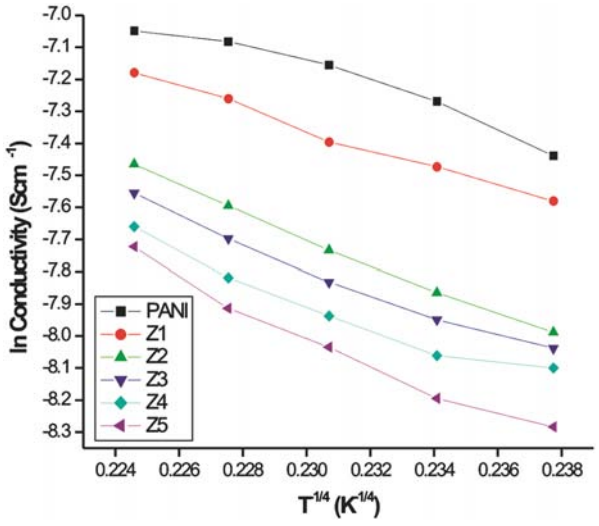

Fig. 10 — Graph between ln (σ_{dc}) versus $T^{-1/4}$ of PANI and PANI/ZnO composites

dimensionality of the conducting medium. The possible values of γ are 1/4, 1/3, 1/2 for three, two and one-dimensional systems, respectively[43]. As seen in Fig. 10, the straight line nature of the lnσ versus $T^{-1/4}$ plots justifies the validity as shown in Fig. (7) for the polyaniline/ZnO composites studied here. The charge conduction is found to be dominated by variable range hopping (VRH) with the three dimensional hopping as shown in Fig. 10. The values of $\ln\sigma_0$ and T_0 obtained from the intercept are obtained from the above mentioned plots and presented in Table 3. The accuracy of the measurement of dc conductivity and hence the parameters listed in Table 3 are of the order of 4%.

4 Conclusions

In summary, the composites of polyaniline with ZnO via oxidative polymerization of aniline hydrochloride in the presence of different wt% of ZnO with ammonium persulphate as an oxidant, have been synthesized. Detailed characterizations of the composites were carried out using XRD, FTIR, TGA, SEM and *dc* conductivity. XRD analysis shows the amorphous nature of the composites. The FTIR analysis confirms the formation of polyaniline and indicates that changes in the polymer structure are due to introduction of zinc oxide in PANI. TGA indicates better thermal stability of composites as compared to PANI. Various kinetic parameters are calculated and their variation with different composition of ZnO in PANI is discussed. The SEM study of PANI/ZnO composites revealed uniform distribution of ZnO particles in PANI matrix.

PANI/ZnO composites show lower *dc* electrical conductivity as compared to PANI and it decreases regularly with increasing content of ZnO. At higher temperatures, *dc* conductivity increases because of hopping of polarons from one localized states to another localized states. As future actions, this work opens new perspectives for the use of PANI/ZnO composites as suitable electronics devices. It is thought that such composites may find important technological applications.

Acknowledgement

Authors are thankful to University Grants Commission (UGC), New Delhi for sanction of major research project no. 41-888/2012 (SR) and Department of science and technology (DST-FIST) for providing financial support.

References

1 Kumar G, Sivasharunugam A, Muniyandi N, Dhawan S K & Trivedi D C, *Svnth Met*, 80 (1996) 279.
2 Saini P & Arora M, *New Polymers for Special Applications* by Gomes A D (ed) Intech, Croatia, 2012.
3 Saini P, Arora M, Gupta G, Gupta B K, Singh V N & Choudhary V, *Nanoscale*, 5 (2013) 4330.
4 Saini P & Arora M, *J Mater Chem A*, 1 (2013) 8926.
5 Saini P, Choudhary V, Singh B P, Mathur R B & Dhawan S K, *Mater Chem Phys*, 113 (2009) 919.
6 Saini P, Choudhary V & Dhawan S K, *Polym Adv Technol*, 20 (2009) 355.
7 Maiti S, Shrivastava N K, Suin S & Khatua B B, *ACS Appl Mater Interfaces*, 5 (2013) 4712.
8 Saini P, Choudhary V, Vijayan N & Kotnala R K, *J Phys Chem C*, 116 (2012) 13403.
9 Saini P & Choudhary V, *J Nanoparticle Res*, 15 (2013) 1415.
10 Saini P & Choudhary V, *J Mater Sci*, 48 (2013) 797.
11 Kumar L, Dhawan S K, Karnalsannan M & Chandra S, *Thin Solid Films,* 411(2003) 243.
12 Tan C K and Blackwood D J, *Corros Sci,* 45 (2003) 545.
13 Salaneck W R, Clark D T & Samuelsen E J, *Sci Applicat conduct polym* (IOP Publishing Ltd., Bristol,UK, 2003).
14 Hwa K, Wha H K Oh & Kang T J, *J Appl Polym sci*, 97 (2005) 1326.
15 Raghavendra S C, Khasim S, Revanasiddappa M, Ambika Prasad M V N & Kulkarni A B, *Bull Mater Sci*, 26 (2003) 733.
16 Pud A, Ogurtsov N, Korzhenko A & Shapoval G, *Prog Polym Sci,* 28 (2003) 1701.
17 Long Y, Chen Z, Wang N, Li J & Wan M, *Physica B: Condensed Matter*, 344 (2004) 82.
18 Chen R, Zou C, Yan X & Gao W, *Prog in Nat Sci: Materials International*, 21 (2011) 81.
19 Huang X H, Xia X H, Yuan Y F & Zhou F, *Electrochim Acta,* 56 (2011) 4960.
20 Phan D T & Chung G S, *Curr App Phys*, 12 (2012) 521.
21 Yumak T, Kuralay F, Muti M, Sinag A, Erdem A & Abaci S, *Colloid Surface B*, 86 (2011) 397.
22 Zhang D, Lee S K, Chava S, Berven C A & Katkanant V, *Physica B*, 406 (2011) 3768.
23 Yun D Q, Xia X Y, Zhang S, Bian Z Q, Liu R H & Huang C H, *Chem Phys Lett*, 516 (2011) 92.
24 Goyal S L, Sharma S, Kumar D & Kishore N, *AIP Conf Proc*, Vol 1536, 2013, p. 799.
25 Chen S A, Chung K R, Chao C L & Lee H T, *Synth Met*, 82 (1996) 207.
26 Vaezi M R, *Mater Design*, 28 (2007) 1065.
27 Dumitrescu I, Nicolae C A, Mocioiu A M, Gabor R A, Grigorescu M & Mihailescu M, *UPB Sci Bull*, 71 (2009) 63.
28 Nouh S A, Atta M R & EL-Melleegy W M, *Radiat Eff Defect S*, 159 (2004) 461.
29 Kalsi P C, Mudher K D S, Pandey A K & Iyer R H, *Thermochim Acta*, 254 (1995) 331.
30 Jellinek H H G, *Aspects of Degradation and Stabilization of Polymers* (Elsevier Scientific Publishing Company: New York, 1978).
31 Singh B K, Kumari P, Prakash A & Adhikari D, *Nat Sci*, 7 (2009) 73.
32 Horowitz H H & Metzger G, *Anal Chem*, 35 (1963) 1464.

33 Mallikarjun K G, *European J Chem*, 1 (2004) 105.
34 ChanshettyV B, Sangshetty K & Sharanappa G, *Int J Eng Res App*, 2 (2012) 611.
35 Singla M L, Awasthi S & Srivastava A, *Sensor Actuat A*, 136 (2007) 604.
36 Gupta R, Kumar V, Goyal P K, Kumar S, Kalsi P C & Goyal S L, *Adv App Sci Res*, 2 (2011) 248.
37 Reghu M, Cao Y, Moses D & Heeger A J, *Phys Rev Lett B*, 47 (1993) 1758.
38 Asha, Goyal S L, Kumar D, Kumar S & Kishore N, *Indian J Pure & Appl Phys,* 52 (2014) 341.
39 Jain N, Patidar D, Saxena N S & Sharma K, *Indian J Pure & Appl Phys*, 44 (2006) 767.
40 Shaktawat V, Jain N, Saxena S, Saxena N S, Sharma K & Sharma T P, *Indian J Pure & Appl Phys*, 46 (2008) 427.
41 Majid K, Awasthi S & Singla M L, *Sensor Actuat A: Physical*, 135 (2007) 113.
42 Dutta P, Biswas S, Ghosh M, De S K & Chatterjee S, *Synth Met*, 122 (200) 455.
43 Mott N F & Davis E A, *Electronic Processes in Non-Crystalline Materials* (Oxford University Press: London 1979).